Supporting Information

W-band orientation selective DEER measurements on a Gd^{3+}/nitroxide mixed-labeled protein dimer with a dual mode cavity

Ilia Kaminker, Igor Tkach, Nurit Manukovsky, Thomas Huber, Hiromasa Yagi, Gottfried Otting, Marina Bennati, and Daniella Goldfarb

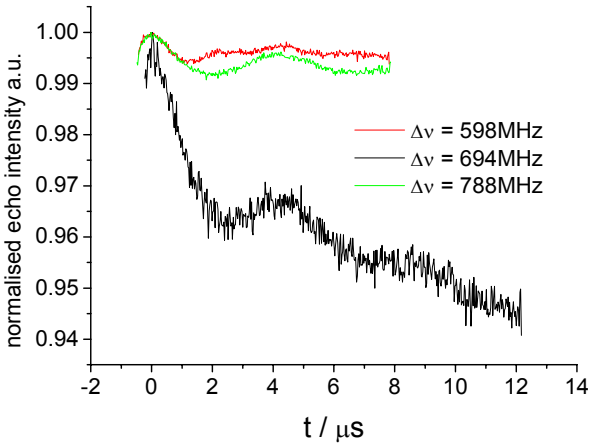

Fig. S1. Raw DEER time domain traces of mixed labeled ERp29 dimers at 10 K.

Simulation of the orientation selective FT-DEER spectra

The FT-DEER spectra were simulated using a home-written MATLAB program for the simulation of the dipolar spectrum under orientation-selective conditions. It is based on the approach presented by Abé *et al.* [1] and modified for the case of orientation selectivity induced by the pumped spins only. The program calculates the dipolar spectrum for an effective spin ½ with an isotropic *g* tensor (corresponding to the central transition of Gd^{3+}) coupled to a nitroxide, with the two electron spins having a given distribution of inter-spin distances and relative orientations.

The axes system used for the simulation is shown in Fig. S2. The axes are chosen to coincide with those of the nitroxide *g*-tensor principal axes system, where the x axis is along the N–O bond, the z axis is along the nitrogen p-orbital and the y-axis is orthogonal to the other two. The nitroxide ^{14}N hyperfine tensor principal axes frame coincides with that of the *g* tensor, with A_{zz} being along g_z. The magnetic field orientation with respect to the nitroxide frame is given by the polar angle θ_0 and the azimuth angle ϕ_0. Likewise, the inter-spin vector orientation with respect to the nitroxide frame is defined by θ and ϕ (Figure S2). The isotropic *g* tensor of Gd^{3+} dispenses with the need for a frame for Gd^{3+}, thereby reducing the complexity [2].

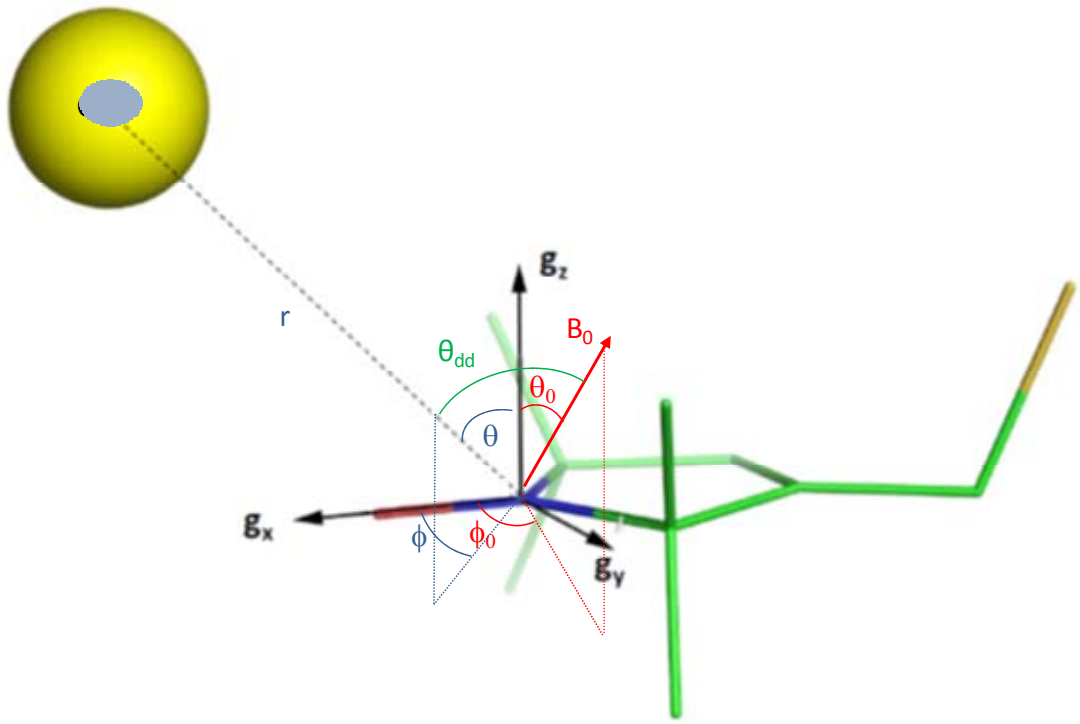

Fig. S2. The axes system and angles used in the simulation. The g-tensor principal axes frame within the MTSL tag is defined by g_z along the N lone pair (which is perpendicular to the planar O-N-$(C)_2$ group), g_x along the N-O bond, and g_y perpendicular to g_x-g_z plane. B_0 is the magnetic field, which is related to the nitroxide frame by the polar angle θ_0 and azimuth angle ϕ_0. ***r*** is the inter-spin vector, with polar angle θ and azimuth angle ϕ with respect to the nitroxide frame. θ_{dd} is the dipolar angle.

The dipolar angle θ_{dd} can be obtained from the scalar product of $\boldsymbol{B_0}$ and ***r***. Hence, for every $\boldsymbol{B_0}$ orientation given by θ_0 and ϕ_0, and a particular geometry defined by ***r***, θ and ϕ, θ_{dd} is calculated followed by the calculation of the dipolar frequency according to [3]:

$$\nu_{dd} = \frac{g_{Gd} g_{NO}^{eff} \mu_0 \beta^2}{8\pi^2 \hbar} \cdot \frac{\left(3\cos^2\theta_{dd} - 1\right)}{r^3} \qquad \text{(S1)}$$

where $g_{Gd} = 1.9923$ is the Gd^{3+} *g*-factor,

$g_{NO}^{eff} = \sqrt{\left(g_x \sin\theta_0 \cos\phi_0\right)^2 + \left(g_y \sin\theta_0 \sin\phi_0\right)^2 + \left(g_z \cos\theta_0\right)^2}$ is the effective *g* factor of the nitroxide for the field orientation at hand, with the nitroxide *g*-tensor principal values (g_x g_y g_z) = (2.0092 2.007 2.003) found by fitting the W-band nitroxide spectrum (data not shown), μ_0 is the vacuum permeability, β is Bohr's magneton, $\hbar$ is the reduced Planck constant, and *r* is the inter-spin distance. The ^{14}N hyperfine principal values used for the simulations were A (NO) = [12.61 12.61 98.09] MHz.

A field-orientation grid was generated by sampling θ_0 and ϕ_0 in 3° intervals each in the range of [0, 180°]. Every possible pair of θ_0 and ϕ_0 defines three resonant

magnetic fields, $B_{res,i}$ (i = 1-3), corresponding to each of the allowed EPR transitions determined by the EasySpin [4] resfields function. The degree to which any of these transitions is excited by the pump pulse, termed $W(B_{res,i})$, was determined by its location within the pump pulse excitation profile. The latter was assumed to follow a Gaussian distribution [5] centered at the pump pulse excitation field B_{pump} with the width (3 standard deviations) ΔB_{pump}. B_{pump} and ΔB_{pump} are the field equivalents of the pump frequency, ν_{pump}, and $\Delta\nu_{pump} = 1/t_p$, where t_p denotes the pump pulse duration (64 ns):

$$W(B_{res,i}) = \exp\left[\frac{-(B_{res,i} - B_{pump})}{2(\frac{\Delta B_{pump}}{3})^2}\right] \tag{S2}$$

The excitation bandwidth used was the nominal one ($1/t_p$), while the effective one, which is broader due to *g* strain and unresolved proton hyperfine interactions, was not used since attempts to broaden the excitation bandwidth from $1/t_p$ to values up to $3/t_p$ did not improve the fit quality.

The excitation degrees of the three transitions belonging to a given field orientation were summed while weighing them by their individual transition probabilities. The resulting excitation degree was then multiplied by the weighting factor $\sin\theta_0$ to yield the final weight of each field orientation:

$$I(\theta_0,\phi_0) = \sum_{i=1,2,3} W\left[B_{res,i}(\theta_0,\phi_0)\right]\cdot P\left[B_{res,i}(\theta_0,\phi_0)\right]\cdot \sin\theta_0 d\theta_0 \tag{S3}$$

where the first term is the extent of pump pulse excitation of a given transition (Eq. S2), dependent on the field orientation and on the nuclear spin manifold, and the second term is the corresponding transition probability.

A molecular geometry grid was generated by sampling θ and ϕ in 9° intervals each and *r* in 0.1 nm intervals. Every triplet of *r*, θ, and ϕ defines a single molecule geometry. These three parameters were assumed to have Gaussian distributions and to be uncorrelated with each other. A grid search was performed for the distribution center and its FWHM (full width at half maximum height) of each variable, resulting in a total of six fitting parameters. The distances tested ranged from 5.7 to 5.9 nm, as this range was suggested by the main peak in the distance distribution obtained by the Tikhonov regularization procedure for the average of the time domain traces and from the frequencies of the singularities in the FT-DEER spectra (see main text for details). To avoid unnecessary computations, we used the fact that the experimental results indicate that the dipolar vector is in the xy plane of the g- principal axis system, with a preference for the x axis. Therefore, the angular distributions tested were centered at θ~60-90° and ϕ~0-20° (equivalent to 180-200°), the latter with a broad distribution (FWHM >100°). For every distribution, there is a set of possible geometries, whose individual weights are dictated by the distribution at hand as products of the weights of the respective *r*, θ and ϕ values.

The dipolar frequency was calculated for every combination of molecular geometry and field orientation using eq. S1. The calculated dipolar frequencies were each convoluted with a Gaussian peak of FWHM = 0.1 MHz and their intensities were weighted by the geometry distribution and the orientational weight at hand. Subsequently, the weighted spectra of all combinations of orientations and geometries were summed to yield a single spectrum associated with a single geometry distribution for each of the three experiments. The individual spectra were normalized setting their maximum intensity to 1.

To find the geometry distribution yielding the best fit to the experimental data, the root mean square deviation (RMSD) of each simulated spectrum was calculated with respect to the corresponding experimental spectrum, including only the frequency ranges [-0.59, -0.12] and [0.12, 0.59] MHz. The frequencies in the range [-0.12, 0.12] MHz were excluded from the RMSD calculation due to the sensitivity of this part of the spectrum to baseline correction. The frequencies above 0.6 MHz or below -0.6 MHz were also excluded, as they are inaccessible to the distances covered by the simulations. Finally, the RMSDs from the three experiments were summed for each tested geometry distribution to obtain the global RMSD, whose minimum was chosen as the geometry yielding the best agreement between the simulation and the experiment. The spectra corresponding to that geometry were recalculated using a finer geometry grid (0.01 nm steps for r, 3° for θ and ϕ).

Determination of the probability distribution of θ and ϕ using molecular modeling.

To assess the accuracy of the orientational selection, we modeled the θ-ϕ angle distribution by crafting the Gd^{3+} C1 tag in one monomer, and the MTSL tag in the other monomer, onto the cysteine residues 114 of the crystal structure of the ERp29 protein dimer (PDB ID 2QC7), as described previously in [6]. For the Gd^{3+} C1 tag, 1000000 models were generated by randomly varying the χ1 and χ2 angles of the cysteine residue as well as all rotatable bonds between the cysteine sulfur atoms and the Gd^{3+} chelate. For the MTSL tag, 200000 models were generated by randomly varying the χ1 and χ2 angles of the cysteine residue as well as all rotatable bonds between the cysteine sulfur atoms and the 2,2,5,5-tetramethyl-2,5-dihydro-1H-pyrrol. Models with van der Waals violations between the tags and the protein were removed, resulting in 15562 Gd^{3+} C1 tag conformations, and 19258 MTSL tag conformations. For each combination of modeled tag conformations, the g-tensor frame of the MTSL tag is calculated. θ and ϕ are the polar angles of the vector between the nitroxide-Gd^{3+} spins with respect to the g-tensor frame (see Fig. S2). θ-ϕ angle distributions were calculated from all $2.99*10^8$ pairwise combinations of tag conformations.

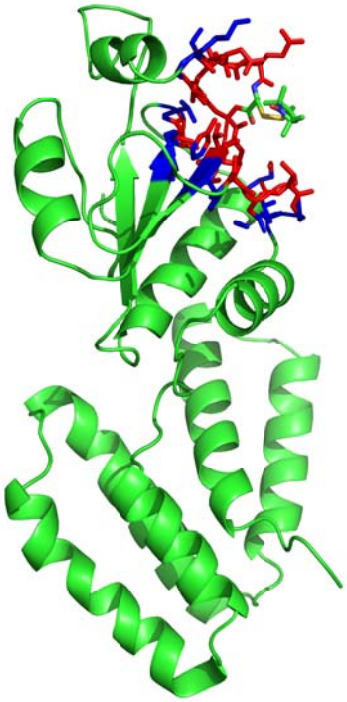

Fig. S3 The ERp29 structure with one rotamer of the MTSL tag and residues coloured red (blue) within 8 (10) Å of the MTSL tag.

[1] C. Abé, D. Klose, F. Dietrich, W.H. Ziegler, Y. Polyhach, G. Jeschke, et al., Orientation selective DEER measurements on vinculin tail at X-band frequencies reveal spin label orientations, Journal of Magnetic Resonance. 216 (2012) 53–61.

[2] D. Goldfarb, Metal-Based Spin Labeling for Distance Determination, in: Structure & Bonding, Springer, Berlin, 2012: pp. 1–42.

[3] G. Jeschke, Y. Polyhach, Distance measurements on spin-labelled biomacromolecules by pulsed electron paramagnetic resonance, Phys. Chem. Chem. Phys. 9 (2007) 1895–1910.

[4] S. Stoll, A. Schweiger, EasySpin, a comprehensive software package for spectral simulation and analysis in EPR, Journal of Magnetic Resonance. 178 (2006) 42–55.

[5] Y. Polyhach, A. Godt, C. Bauer, G. Jeschke, Spin pair geometry revealed by high-field DEER in the presence of conformational distributions, Journal of Magnetic Resonance. 185 (2007) 118–129.

[6] I. Kaminker, H. Yagi, T. Huber, A. Feintuch, G. Otting, D. Goldfarb, Spectroscopic selection of distance measurements in a protein dimer with mixed nitroxide and Gd^{3+} spin labels, Phys. Chem. Chem. Phys. 14 (2012) 4355–4358.